

# Charm Production as a Function of Energy

R. Vogt

Lawrence Livermore National Laboratory, Livermore, CA 94551, USA

Physics Department, University of California, Davis, CA 95616, USA

# Charm Hadrons

Open charm hadron decays can be detected both through lepton channels (semi-leptonic decays) and pure hadronic channels ( $D$  mass, momentum reconstruction)  
 Measuring  $D$  mesons alone is not enough to get total  $c\bar{c}$  cross section

$C$	Mass (GeV)	$c\tau$ ( $\mu\text{m}$ )	$B(C \rightarrow lX)$ (%)	$B(C \rightarrow \text{Hadrons})$ (%)
$D^+(c\bar{d})$	1.869	315	17.2	$K^-\pi^+\pi^+$ (9.1)
$D^-(\bar{c}d)$	1.869	315	17.2	$K^+\pi^-\pi^-$ (9.1)
$D^0(c\bar{u})$	1.864	123.4	6.87	$K^-\pi^+$ (3.8)
$\bar{D}^0(\bar{c}u)$	1.864	123.4	6.87	$K^+\pi^-$ (3.8)
$D^{*\pm}$	2.010			$D^0\pi^\pm$ (67.7), $D^\pm\pi^0$ (30.7)
$D^{*0}$	2.007			$D^0\pi^0$ (61.9)
$D_s^+(c\bar{s})$	1.969	147	8	$K^+K^-\pi^+$ (4.4), $\pi^+\pi^+\pi^-$ (1.01)
$D_s^-(\bar{c}s)$	1.969	147	8	$K^+K^-\pi^-$ (4.4), $\pi^+\pi^-\pi^-$ (1.01)
$\Lambda_c^+(udc)$	2.285	59.9	4.5	$\Lambda X$ (35), $pK^-\pi^+$ (2.8)
$\Sigma_c^{++}(uuc)$	2.452			$\Lambda_c^+\pi^+$ (100)
$\Sigma_c^+(udc)$	2.451			$\Lambda_c^+\pi^0$ (100)
$\Sigma_c^0(ddc)$	2.452			$\Lambda_c^+\pi^-$ (100)
$\Xi_c^+(usc)$	2.466	132		$\Sigma^+K^-\pi^+$ (1.18)
$\Xi_c^0(dsc)$	2.472	29		$\Xi^-\pi^+$ (seen)

Table 1: Ground state charm hadrons with their mass, decay length (when given) and branching ratios to leptons (when applicable) and some prominent decays to hadrons, preferably to only charged hadrons although such decays are not always available.

# Experiments Measure Different Parts of Phase Space

## Fixed Target Experiments

Longitudinal momentum fraction,  $x_F$ , is a useful observable,  $x_F = 2p_L/\sqrt{S} = 2m_T \sinh y/\sqrt{S}$

Bubble chambers cover forward region,  $x_F = 2p_L/\sqrt{S} = 2m_T \sinh y/\sqrt{S} > 0$

Beam dumps measured either  $\nu$  or  $\mu$ : proton beam dumped onto a dense target which suppresses  $\pi$  and  $K$  decays so that, when density is high enough, charm is only remaining lepton source

Extrapolate to infinite density to relate  $\nu$  and  $\mu$  flux to the  $c\bar{c}$  cross section

Data at forward  $x_F$ , charm not directly reconstructed, momentum is uncertain

## ISR Collider Experiments

ISR experiments, at  $\sqrt{S} = 53 - 63$  GeV, covered small part of phase space so results heavily dependent on extrapolation to full phase space

Some results from dileptons, others from an electron trigger and a reconstructed charm hadron

Dileptons ( $e^\pm\mu^\mp$ ,  $e^+e^-$  and  $\mu^+\mu^-$ ) give most reasonable cross sections,  $\sigma < 100 \mu\text{b}$

Hadron channel results assumed  $pp \rightarrow \bar{D}\Lambda_c X$  characterized by  $dN/dx_F \sim (1 - x_F)^n$

Detected a charm decay electron opposite a reconstructed  $\Lambda_c \rightarrow Kp\pi$  or  $D \rightarrow K\pi\pi$

With  $x_F$  distribution assumed to go like  $n \sim 0$  or  $n \sim 3$ ,  $\sigma \geq 500 \mu\text{b}$

## Modern Era

Most recent fixed-target and collider experiments use silicon detectors placed near target, easier to reconstruct hadron momentum but  $x_F$  ( $y$ ) range more limited

If cross section measurable for  $p_T > 0$ , then NLO pQCD cross section calculations make extrapolation to full phase space more reliable than previously

Tevatron measurements of  $D^+$ ,  $D^0$  and  $D_s$  at  $p_T > 5$  GeV, not possible to extrapolate down to obtain total cross section, detectors cover central unit of rapidity

RHIC detectors can cover more of phase space and reach lower  $p_T$  than proton colliders to obtain total cross section:

STAR can reconstruct  $D^0$  decays;

PHENIX covers forward and backward rapidity regions up to  $y \sim 2.4$  with muons;

Both have electron measurements at central rapidities

LHC: ALICE plans to measure  $D^0$  decays to low  $p_T$ , CMS and ATLAS can measure heavy flavors with muons

# Obtaining the Total Charm Cross Section from Data

To go from the  $D$  measurement (experiment) to the total charm cross section (theory calculation) we need to know how to extrapolate to full phase space and all charm hadrons

Accurate knowledge of decay branching ratios needed, some old measurements used significantly different branching ratios than those used today

Ideally the number of “signal” charm counts determines the minimum bias cross section

$$N_D = \sigma_D L t$$

where  $Lt$  is the luminosity over run time

Add up all the cross sections for measured  $D$  states,  $D^+$ ,  $D^0$  and their conjugates and correct for the unmeasured part, *e.g.* if coverage is  $x_F > 0$ , a calculated factor of 1.6 (pions) or 2 (protons) is needed to extrapolate to all  $x_F$

$$\sigma_{c\bar{c}} = X \frac{\sigma_{D^+} + \sigma_{D^0} + \sigma_{D^-} + \sigma_{\bar{D}^0}}{2}$$

Pair cross section is half the sum of the single hadron cross sections

Unmeasured part of total charm cross section represented by  $X \sim 1.2-1.5$  to account for  $D_s$  ( $\approx 20\%$ ) and  $\Lambda_c$  ( $\approx 30\%$ ) production (S. Aoki *et al.*, *Prog. Theor. Phys.* **87** (1992) 1305)

# A Dependence

Many fixed-target experiments used nuclear targets to enhance statistics

A dependence of hard and soft processes are not the same — charm is assumed to be a hard process

Total cross section A dependence parameterized as

$$\sigma_{pA} = \sigma_{pp}A^\alpha, \quad \sigma_{AB} = \sigma_{pp}(AB)^\alpha$$

For hard processes,  $\alpha \approx 1$ , but nuclear effects tend to make  $\alpha < 1$ , albeit not by much for integrated cross section

A dependence comes from integration over impact parameter, related to nuclear thickness function,  $T_A = \int dz \rho_A(b, z)$ , in pA, number of binary collisions in AB,

$$N_{\text{coll}}(b) = \sigma_{NN} \int d^2s T_A(s) T_B(|\vec{b} - \vec{s}|),$$

$$\int d^2b T_A(b) = A, \quad \int d^2b d^2s T_A(s) T_B(|\vec{b} - \vec{s}|) = AB$$

Dividing  $\sigma_{pA}$  ( $\sigma_{AB}$ ) by A (AB) gives the per nucleon cross section

$\alpha$  may drop with  $x_F$ , some indication of this from beam dump experiments

The A dependence of soft processes differs,

$$\alpha(x_F \sim 0) \approx 0.7, \quad \alpha(x_F \sim 0.8) \approx 0.5$$

Soft behavior is seen for  $p \rightarrow \pi, p, K, \Lambda$  with  $\alpha = 0.72$  in minimum bias collisions

Some early experiments assumed D production was a soft process

# Calculating Heavy Flavors in Perturbative QCD

‘Hard’ processes have a large scale in the calculation that makes perturbative QCD applicable: high momentum transfer,  $\mu^2$ , high mass,  $m$ , high transverse momentum,  $p_T$ , since  $m \neq 0$ , heavy quark production is a ‘hard’ process

Asymptotic freedom assumed to calculate the interactions between two hadrons on the quark/gluon level but the confinement scale determines the probability of finding the interacting parton in the initial hadron

Factorization assumed between perturbative, calculable hard scattering and the universal, nonperturbative parton distribution functions

Hadronic cross section in an  $AB$  collision where  $AB = pp, pA$  or nucleus-nucleus is

$$\sigma_{AB}(S, m^2) = \sum_{i,j=q,\bar{q},g} \int_{4m_Q^2/s}^1 \frac{d\tau}{\tau} \int dx_1 dx_2 \delta(x_1 x_2 - \tau) f_i^A(x_1, \mu_F^2) f_j^B(x_2, \mu_F^2) \widehat{\sigma}_{ij}(s, m^2, \mu_F^2, \mu_R^2)$$

$f_i^A$  are the nonperturbative parton distributions, determined from fits to data,  $x_1$  and  $x_2$  are the fractional momentum of hadrons  $A$  and  $B$  carried by partons  $i$  and  $j$ ,  $\tau = s/S$

$\widehat{\sigma}_{ij}(s, m^2, \mu_F^2, \mu_R^2)$  is hard partonic cross section calculable in QCD in powers of  $\alpha_s^{2+n}$ : leading order (LO),  $n = 0$ ; next-to-leading order (NLO),  $n = 1 \dots$

Results depend strongly on quark mass,  $m$ , factorization scale,  $\mu_F$ , in the parton densities and renormalization scale,  $\mu_R$ , in  $\alpha_s$

# Total Cross Sections

Partonic total cross section only depends on quark mass  $m$ , not kinematics  
To NLO

$$\hat{\sigma}_{ij}(s, m, \mu_F^2, \mu_R^2) = \frac{\alpha_s^2(\mu_R^2)}{m^2} \left\{ f_{ij}^{(0,0)}(\rho) + 4\pi\alpha_s(\mu_R^2) \left[ f_{ij}^{(1,0)}(\rho) + f_{ij}^{(1,1)}(\rho) \ln(\mu_F^2/m^2) \right] + \mathcal{O}(\alpha_s^2) \right\}$$

$\rho = 4m^2/s$ ,  $s$  is partonic center of mass energy squared

$\mu_F$  is factorization scale, separates hard part from nonperturbative part

$\mu_R$  is renormalization scale, scale at which strong coupling constant  $\alpha_s$  is evaluated

$\mu_F = \mu_R$  in evaluations of parton densities

$f_{ij}^{(a,b)}$  are dimensionless,  $\mu$ -independent scaling functions,  $a = 0, b = 0$  and  $ij = q\bar{q}, gg$  for LO,  $a = 1, b = 0, 1$  and  $ij = q\bar{q}, gg$  and  $qg, \bar{q}g$  for NLO

$f_{ij}^{(0,0)}$  are always positive,  $f_{ij}^{(1,b)}$  can be negative also

Note that if  $\mu_F^2 = m^2$ ,  $f_{ij}^{(1,1)}$  does not contribute

# Scaling Functions to NLO

Near threshold,  $\sqrt{s}/2m \rightarrow 1$ , Born contribution is large but dies away for  $\sqrt{s}/2m \rightarrow \infty$

At large  $\sqrt{s}/2m$ ,  $gg$  channel is dominant, then  $qg$

**NLO  $gg$  and  $qg$  scaling functions independent of energy at  $\sqrt{s}/2m > 20$**

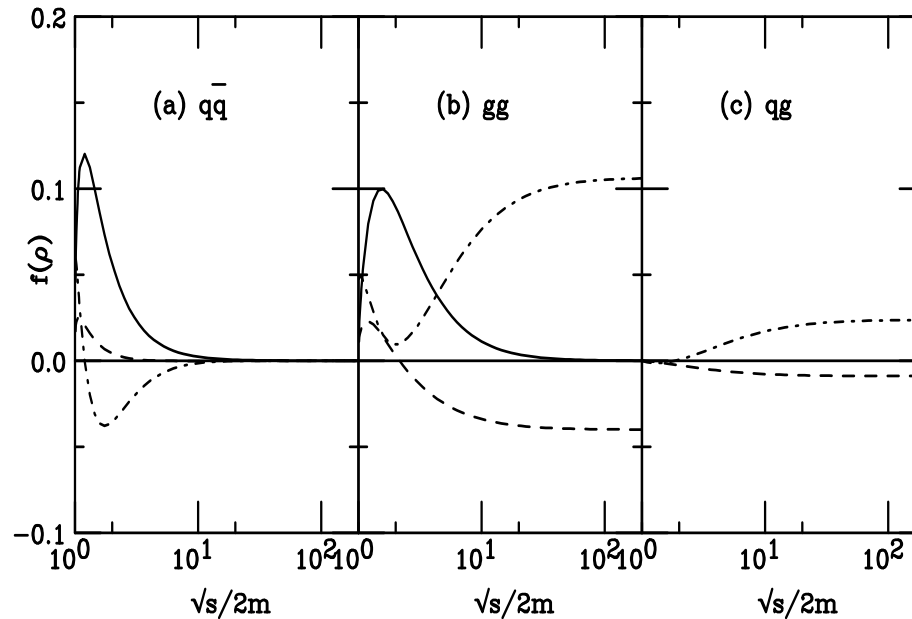


Figure 1: Scaling functions needed to calculate the total partonic  $Q\bar{Q}$  cross section. The solid curves are the Born results,  $f_{ij}^{(0,0)}$ , the dashed and dot-dashed curves are NLO contributions,  $f_{ij}^{(1,1)}$  and  $f_{ij}^{(1,0)}$  respectively.

# Charm Production as a Function of $m$ and $\mu^2$

Keeping  $\mu_F^2 = \mu_R^2 = \mu^2$ , as in parton density fits ( $\mu < m$  not shown)

The  $pp$  data are from reviews by Tavernier (1987), Appel (1992) and later

More recent data favors lower masses

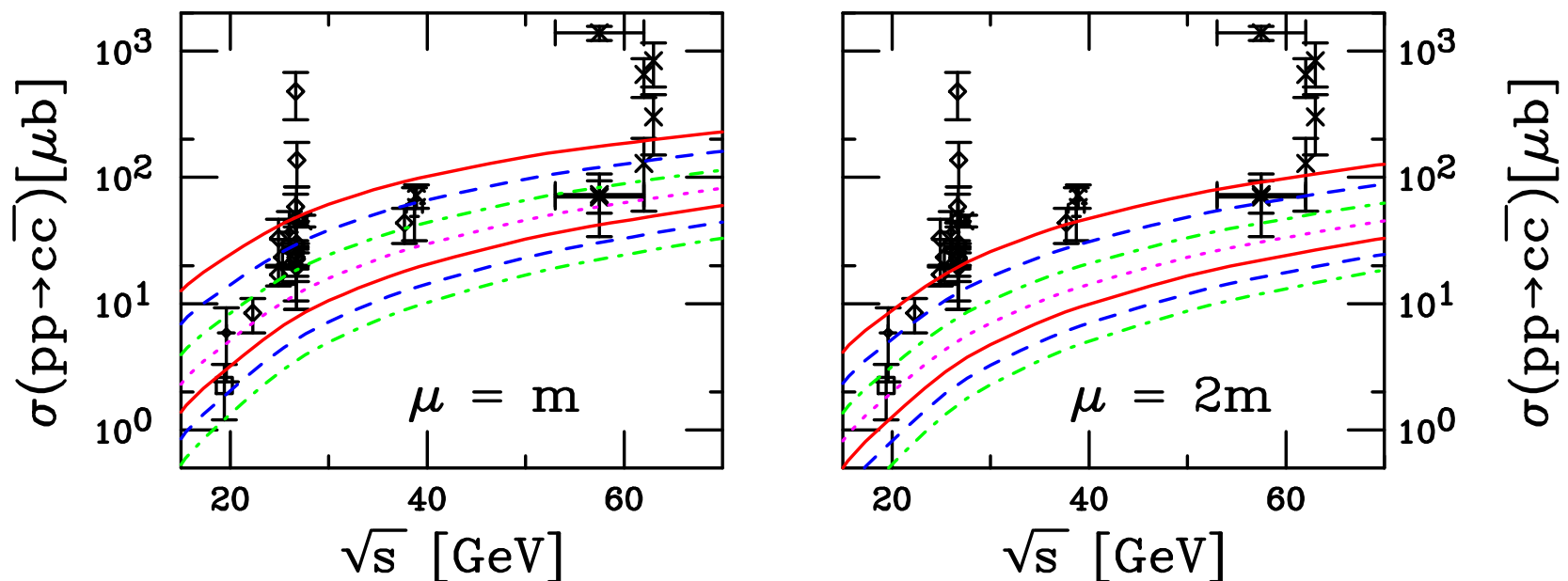


Figure 2: Total  $c\bar{c}$  cross sections in  $pp$  interactions up to ISR energies as a function of the charm quark mass. All calculations are fully NLO using the CTEQ6M parton densities. The left-hand plot shows the results with the  $\mu_R = \mu_F = m$  while in the right-hand plot  $\mu_R = \mu_F = 2m$ . From top to bottom the curves are  $m = 1.2, 1.3, 1.4, 1.5, 1.6, 1.7,$  and  $1.8$  GeV.

## Extrapolation to Higher Energies

Large  $\sqrt{S}$  behavior of  $c\bar{c}$  cross section due to low  $x$  behavior of PDFs and phase space – lower scale closer to minimum  $\mu$  of PDFs, strong factorization scale dependence of gluon density at low  $\mu$

Only most recent measurements shown, including the PHENIX  $\sqrt{S} = 130$  and  $200$  GeV (Au+Au and  $pp$  respectively) results and STAR  $pp$  and d+Au points at  $\sqrt{S} = 200$  GeV

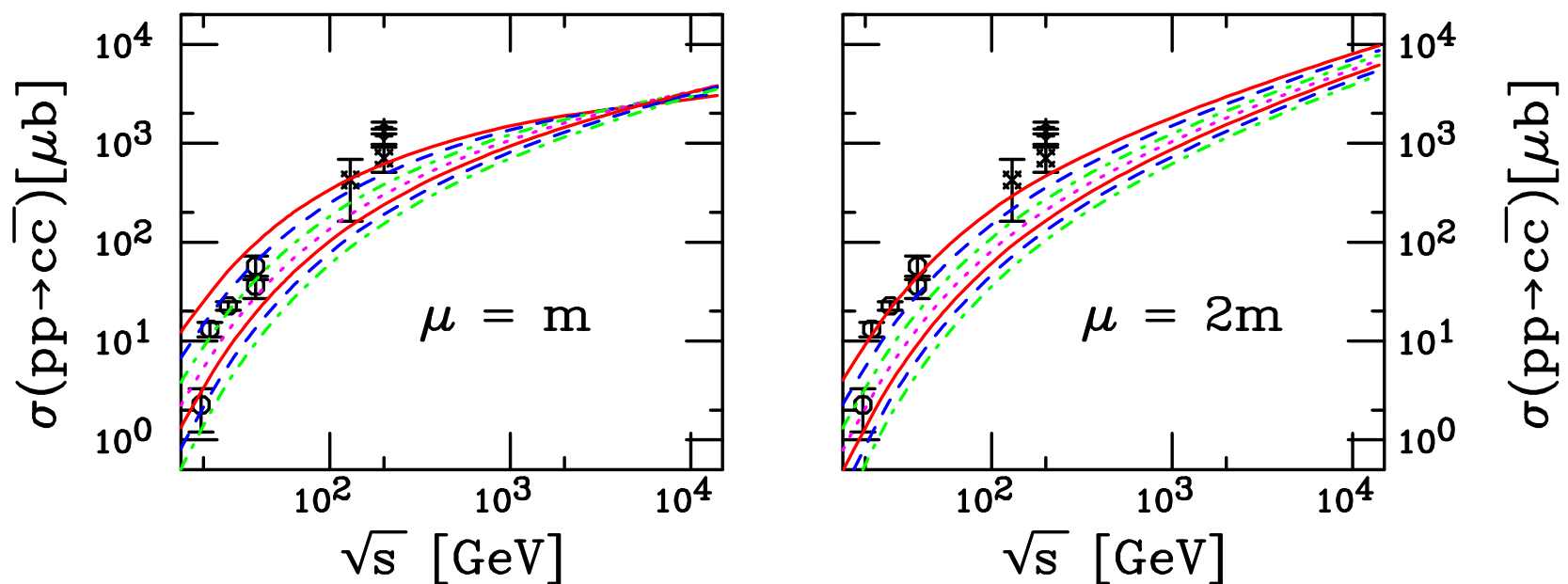


Figure 3: Total  $c\bar{c}$  cross sections in  $pp$  interactions up to 14 TeV with the CTEQ6M PDFs. The left-hand plot shows the results with the  $\mu_R = \mu_F = m$  while in the right-hand plot  $\mu_R = \mu_F = 2m$ . From top to bottom the curves are  $m = 1.2, 1.3, 1.4, 1.5, 1.6, 1.7,$  and  $1.8$  GeV

# Theoretical Uncertainty: Total Charm

Uncertainty band (Cacciari, Nason and RV): from mass range  $1.3 < m < 1.7$  GeV with  $\mu_F = \mu_R = m$ , and scale range relative to central mass value,  $m = 1.5$  GeV –  $(\mu_F/m, \mu_R/m) = (1, 1), (2, 2), (0.5, 0.5), (0.5, 1), (1, 0.5), (1, 2), (2, 1)$

$(\mu_F/m, \mu_R/m) = (1, 0.5)$  and  $(0.5, 0.5)$  have large  $\sigma$  at  $\sqrt{S} < 100$  GeV since  $\alpha_s$  big

At large  $\sqrt{S}$   $(\mu_F/m, \mu_R/m) = (0.5, 0.5), (0.5, 1)$  flattens because  $\mu_F < \mu_0$  of PDF

Evolution faster for combination of small  $x$  and high  $\mu$  [ $(\mu_F/m, \mu_R/m) = (2, 2), (2, 1)$ ]

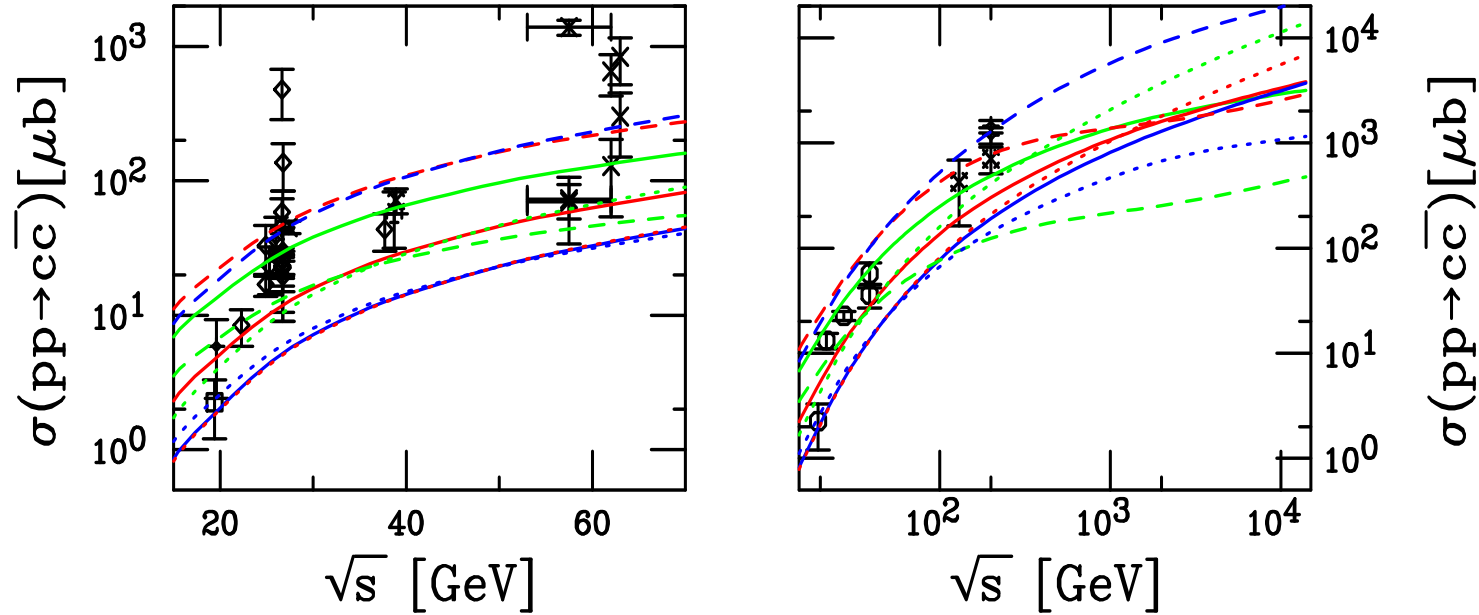


Figure 4: Total  $c\bar{c}$  cross sections calculated using CTEQ6M. The solid red curve is the central value  $(\mu_F/m, \mu_R/m) = (1, 1)$  with  $m = 1.5$  GeV. The green and blue solid curves are  $m = 1.3$  and  $1.7$  GeV with  $(1, 1)$  respectively. The red, blue and green dashed curves correspond to  $(0.5, 0.5), (1, 0.5)$  and  $(0.5, 1)$  while the red, blue and green dotted curves are for  $(2, 2), (1, 2)$  and  $(2, 1)$ , all for  $m = 1.5$  GeV.

# Theoretical Uncertainty Band: Total Bottom

Band narrower for higher mass bottom,  $\mu_F/m = 0.5$  not near initial PDF scale

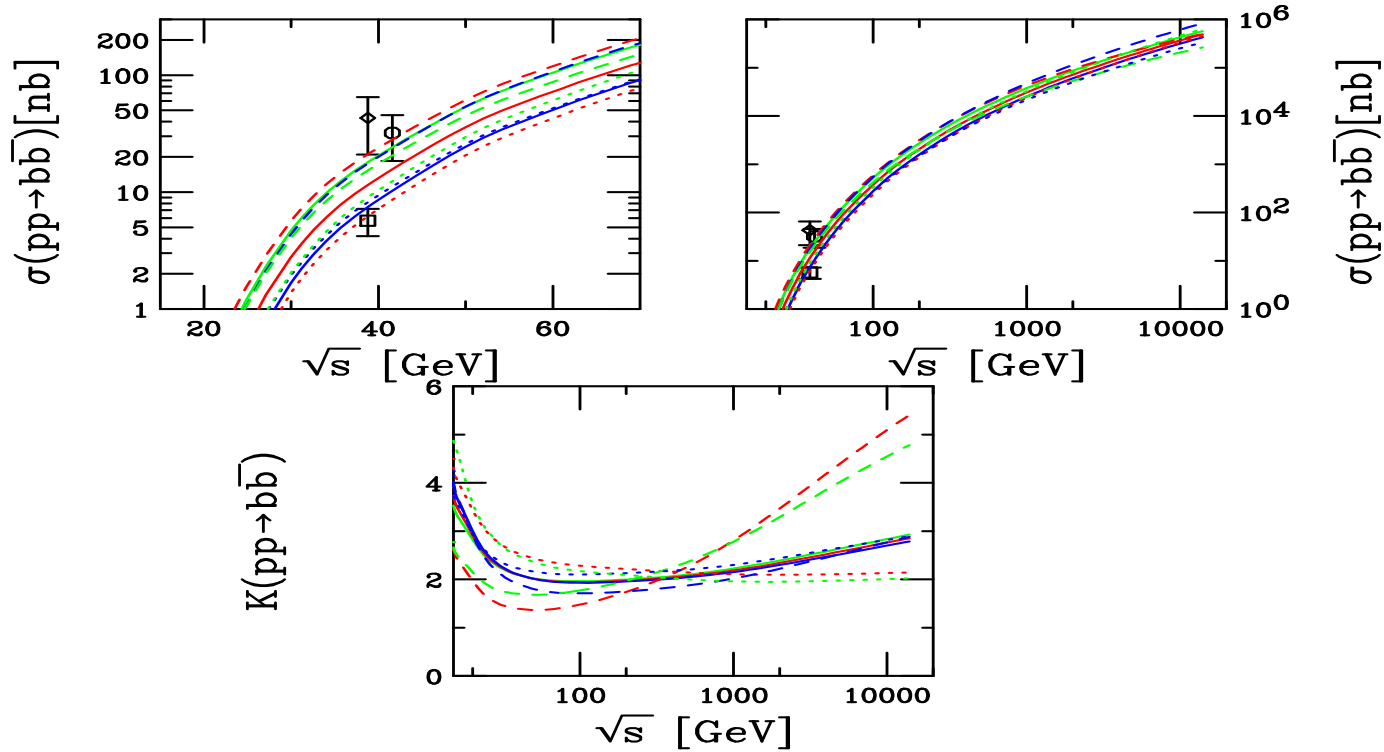


Figure 5: Total  $b\bar{b}$  cross sections calculated using CTEQ6M. The solid red curve is the central value  $(\mu_F/m, \mu_R/m) = (1, 1)$  with  $m = 4.75$  GeV. The green and blue solid curves are  $m = 4.5$  and  $5$  GeV with  $(1, 1)$  respectively. The red, blue and green dashed curves correspond to  $(0.5, 0.5)$ ,  $(1, 0.5)$  and  $(0.5, 1)$  respectively while the red, blue and green dotted curves are for  $(2, 2)$ ,  $(1, 2)$  and  $(2, 1)$  respectively, all for  $m = 4.75$  GeV.

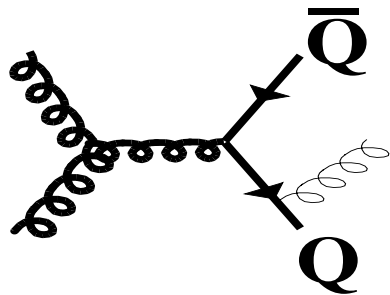
## PYTHIA vs. NLO Calculations

PYTHIA requires separate calculations depending on how many heavy quarks at hard vertex, labeled pair creation (2), flavor excitation (1) and gluon splitting (0) rather than grouping diagrams by initial state as in NLO ( $q\bar{q}$ ,  $gg$ ,  $qg$ )

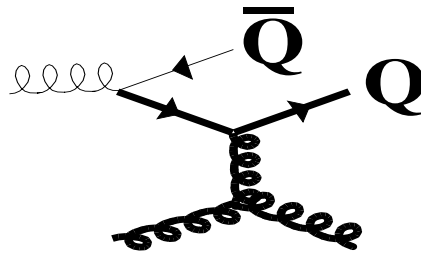
Splitting and excitation are subclasses of  $gg$  and  $qg$  NLO diagrams

PYTHIA typically gives larger cross sections because no interference terms

Pair Creation



Flavour Excitation



Gluon Splitting

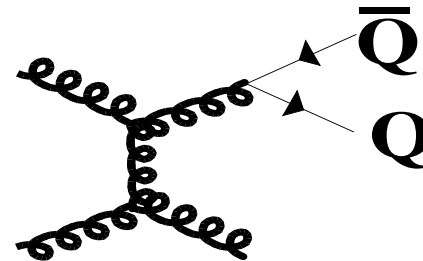


Figure 6: Examples of pair creation, flavor excitation and gluon splitting. The thick lines correspond to the hard process, the thin ones to the parton shower.

# Production Properties in PYTHIA

Pair creation: Two heavy quarks in hard scattering

LO diagrams and (multiple) virtual gluon emission

$Q^2 = m^2 + \hat{p}_\perp$ , massive matrix elements

Flavor excitation: Heavy flavor from parton distribution of beams,  $Qq \rightarrow Qq$ ,

$Qg \rightarrow Qg$

One heavy quark in hard scattering

If  $Q$  is not a valence quark, must be generated from  $g \rightarrow Q\bar{Q}$

$Q^2 = \hat{p}_\perp^2 = \hat{t}\hat{u}/\hat{s}$

Since  $f_Q^p = 0$  for  $Q^2 < m^2$ , massless matrix elements used

Gluon splitting:  $g \rightarrow Q\bar{Q}$  in initial or final state shower, no  $Q$  in hard scattering

Space-like shower:  $Q_{\max}^2 = Q^2 = m^2$  (threshold)

Time-like shower:  $M_{\max}^2 = 4Q^2 = 4m^2$  (threshold)

Parameters CTEQ 5L,  $m_c = 1.5$  GeV,  $m_b = 4.8$  GeV,  $\Lambda_4 = 0.192$  GeV

# Total Charm $\sqrt{s}$ Dependence in PYTHIA Similar to NLO

The trend of the total charm cross section with energy is similar to NLO but, for same parameters, PYTHIA tends to give higher cross section

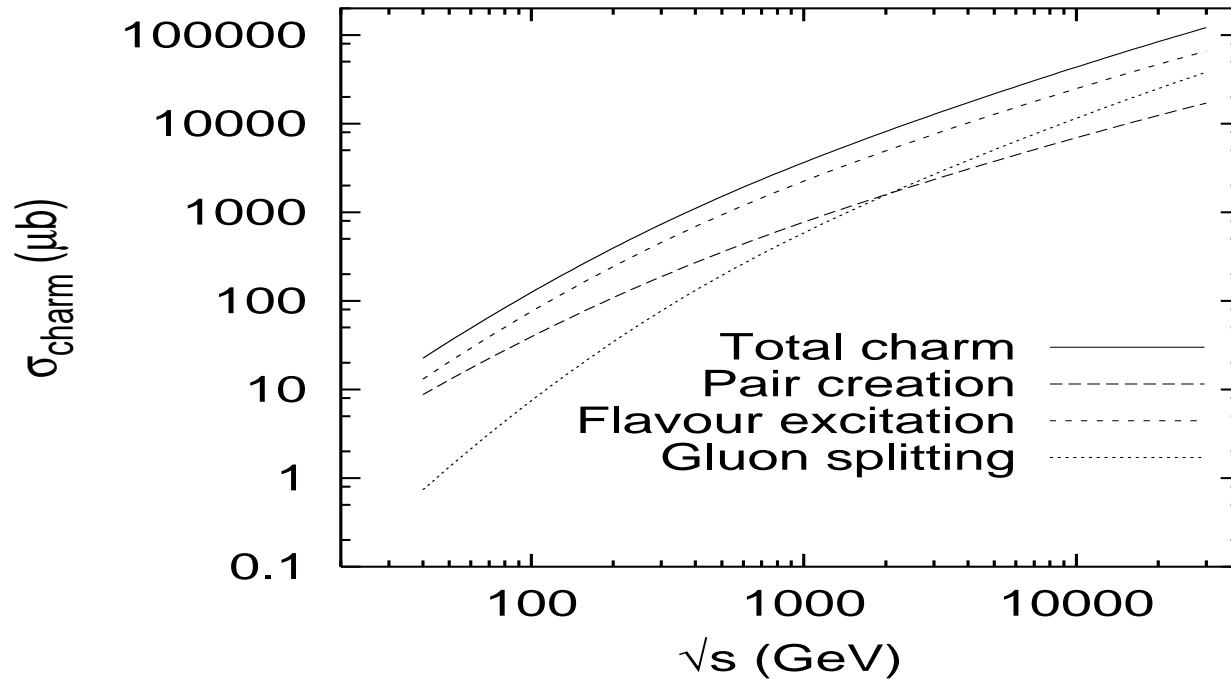


Figure 7: The total charm cross section in  $pp$  interactions with PYTHIA is shown as a function of energy. The long-dashed line is the pair creation contribution, the short-dashed line, flavor excitation, and the dotted line, gluon splitting. The sum of the three contributions is given by the solid line. From Norrbin and Sjostrand, Eur. J. Phys. **C17** (2000) 137.

# At LO Level, Distributions Nearly Identical

Parton showers turned off in PYTHIA and  $k_T$  kick,  $\langle k_T^2 \rangle = 1 \text{ GeV}^2$ , included in PYTHIA and LO calculations

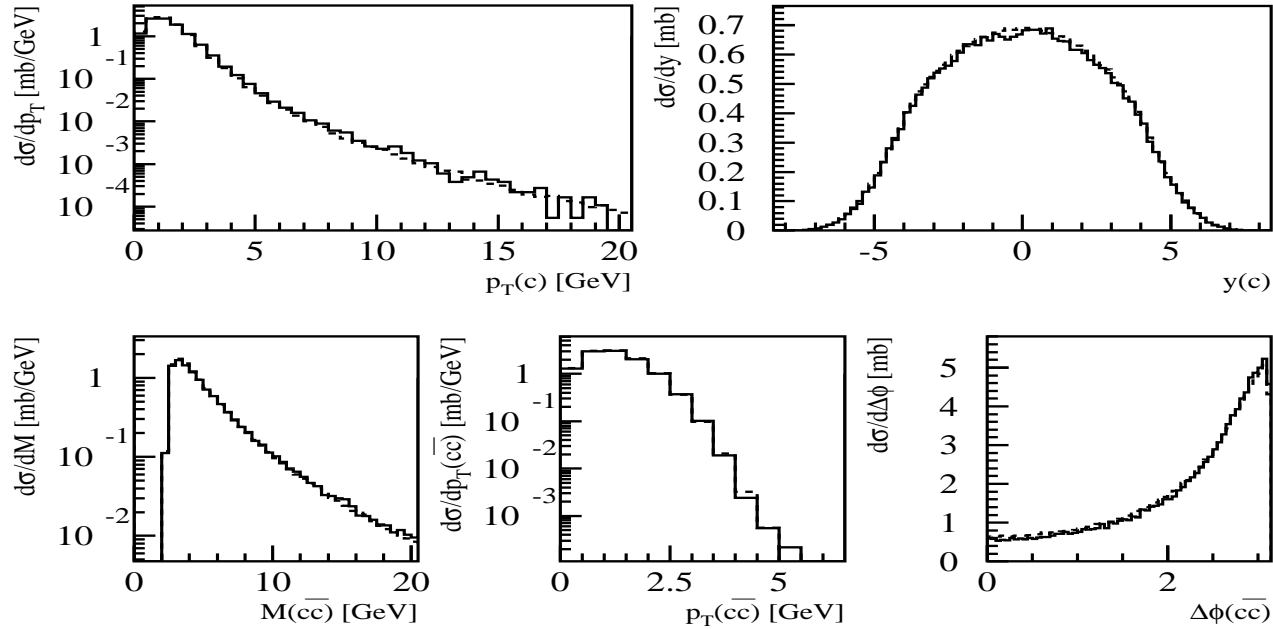


Figure 8: Comparison between PYTHIA results (solid histogram) for  $gg \rightarrow c\bar{c}$ , without parton showers, and the MNR calculation (Nucl. Phys. B xxx) of the same process at LO (dashed histogram) at  $\sqrt{S} = 5.5 \text{ TeV}$ . From arXiv:hep-ph/0311048.

## PYTHIA Parameters Used to Compare to NLO

description	parameter	Charm	Bottom
<b>Process types</b>	MSEL	<b>1</b>	<b>1</b>
<b>Quark mass</b>	PMAS(4/5,1)	<b>1.2</b>	<b>4.75</b>
<b>Minimum <math>p_T^{\text{hard}}</math></b>	CKIN(3)	<b>2.1</b>	<b>2.75</b>
<b>CTEQ4L</b>	MSTP(51)	<b>4032</b>	<b>4032</b>
<b>Proton PDF</b>	MSTP(52)	<b>2</b>	<b>2</b>
<b>No multiple interactions</b>	MSTP(81) PARP(81/82)	<b>0</b> <b>0</b>	<b>0</b> <b>0</b>
<b>Parton showers on</b>	MSTP(61/71)	<b>1</b>	<b>1</b>
<b>2<sup>nd</sup> order <math>\alpha_s</math></b>	MSTP(2)	<b>2</b>	<b>2</b>
<b>QCD scales for hard scattering and parton shower</b>	MSTP(32) PARP(34/67) PARP(71)	<b>2</b> <b>1</b> <b>4</b>	<b>2</b> <b>1</b> <b>1</b>
<b>Intrinsic <math>k_T</math></b>	MSTP(91) PARP(91) PARP(93)	<b>1</b> <b>1.304 (Pb+Pb)</b> <b>1 (<math>pp</math>)</b> <b>6.52 (Pb+Pb)</b> <b>5 (<math>pp</math>)</b>	<b>1</b> <b>2.035 (Pb+Pb)</b> <b>1 (<math>pp</math>)</b> <b>10.17 (Pb+Pb)</b> <b>5 (<math>pp</math>)</b>

Table 2: PYTHIA parameters for  $c$  and  $b$  production in Pb+Pb collisions at  $\sqrt{S_{NN}} = 5.5$  TeV and  $pp$  collisions at  $\sqrt{S} = 14$  TeV. Unspecified parameters are PYTHIA 6.150 defaults.

# Charm Distributions: NLO vs. PYTHIA

Agreement generally rather good, PYTHIA  $\Delta\phi$  distribution peaked more toward  $\pi$  than NLO

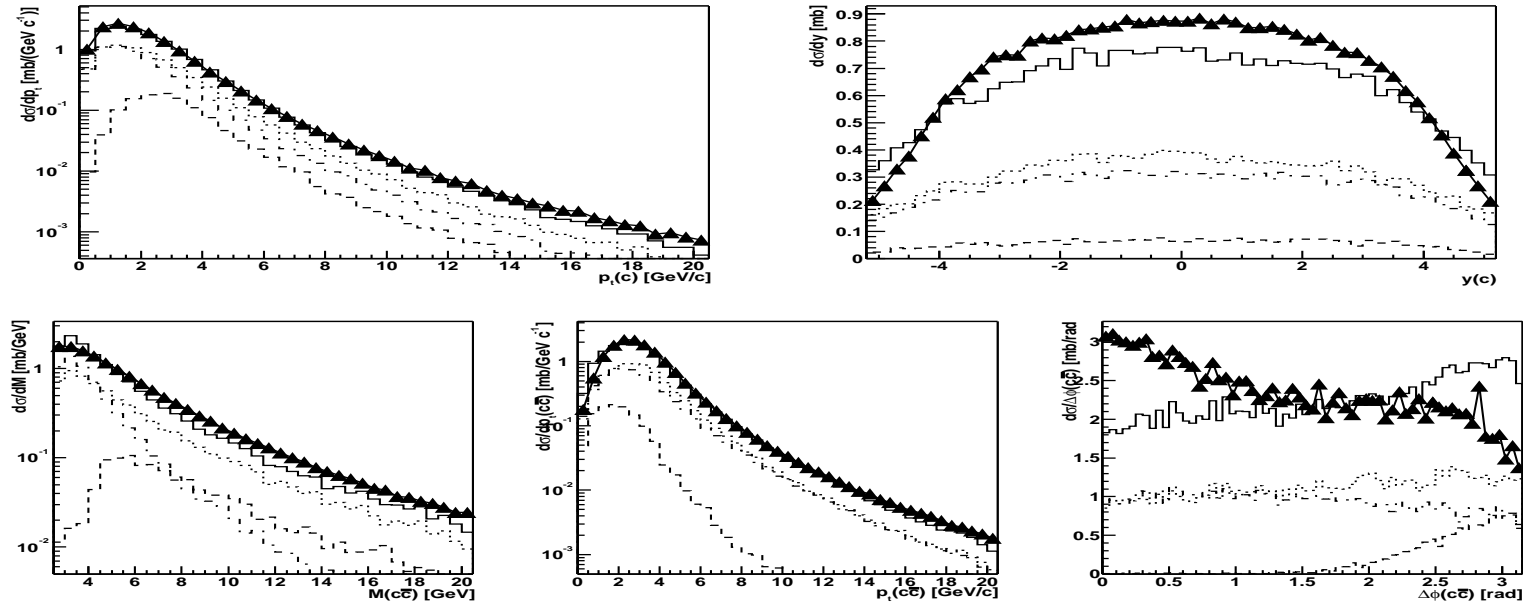


Figure 9: Comparison between charm production in the NLO calculation by Mangano, Nason and Ridolfi and in PYTHIA with parameters tuned as described in the text for Pb+Pb collisions at  $\sqrt{S_{NN}} = 5.5$  TeV. The triangles show the NLO calculation, the solid histogram corresponds to the PYTHIA total production. The individual PYTHIA contributions are flavor creation (dashed), flavour excitation (dotted) and gluon splitting (dot-dashed). From arXiv:hep-ph/0311048.

# Total Bottom $\sqrt{S}$ Dependence Similar to NLO

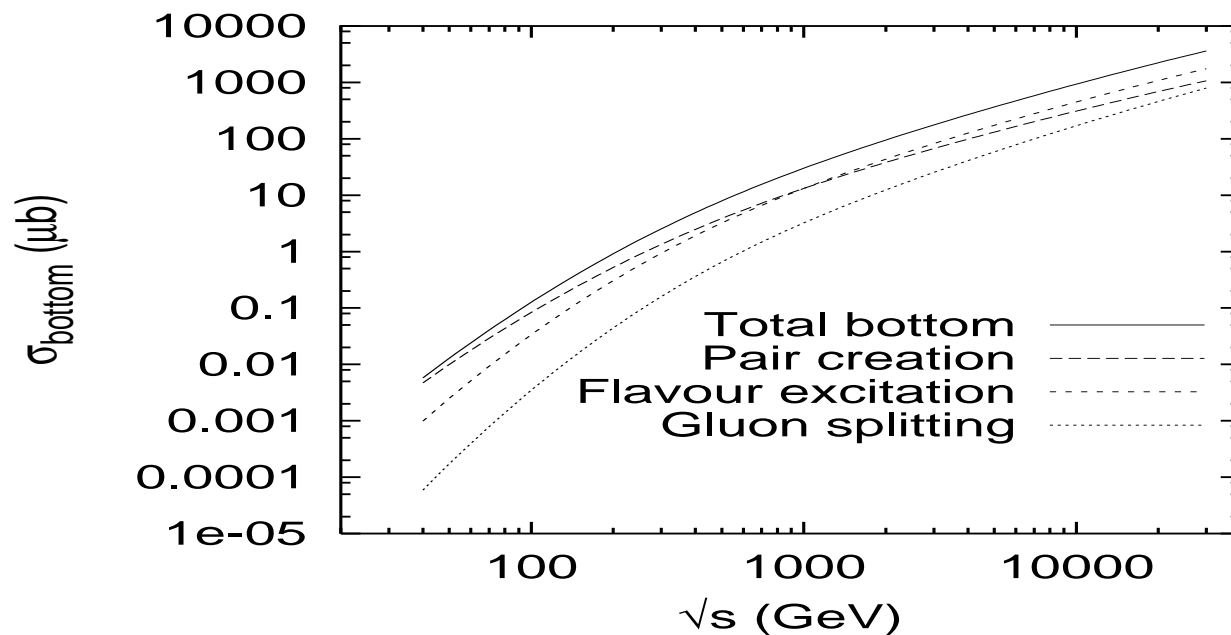


Figure 10: The total bottom cross section in  $pp$  interactions with PYTHIA is shown as a function of energy. The long-dashed line is the pair creation contribution, the short-dashed line, flavor excitation, and the dotted line, gluon splitting. The sum of the three contributions is given by the solid line. From Norrbin and Sjostrand, Eur. J. Phys. **C17** (2000) 137.

# Bottom Distributions: NLO vs. PYTHIA

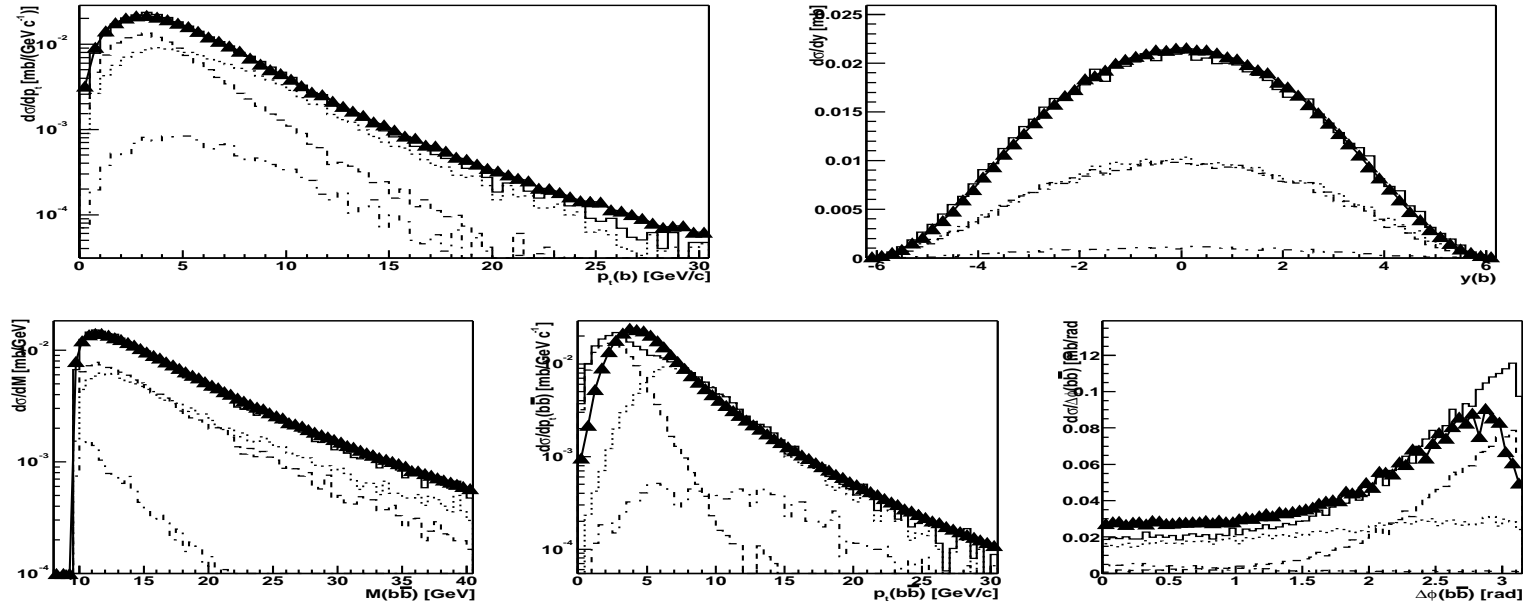


Figure 11: Comparison between bottom production in the NLO calculation by Mangano, Nason and Ridolfi and in PYTHIA with parameters tuned as described in the text for Pb+Pb collisions at  $\sqrt{S_{NN}} = 5.5$  TeV. The triangles show the NLO calculation, the solid histogram corresponds to the PYTHIA total production. The individual PYTHIA contributions are flavor creation (dashed), flavour excitation (dotted) and gluon splitting (dot-dashed). From arXiv:hep-ph/0311048.

# RHIC Results

STAR  $D^0$  and PHENIX/STAR electron  $p_T$  distributions compared to FONLL calculations (Cacciari, Nason and RV)

See Matteo's talk for more about FONLL calculations

$p_T$  distributions include fragmentation functions for  $c \rightarrow D$  and semileptonic decays to electrons,  $D/B \rightarrow eX$

Fragmentation functions consistent with FONLL calculations, harder than typically-used Peterson, more like a delta function

Large uncertainties in total cross section less important here for  $p_T > 1.5m$  since by then  $\mu \propto m_T$  is always larger than minimum scale of PDF, reducing PDF uncertainty

# Uncertainty Bands for $c$ and $b$ at 200 GeV

Not possible to separate  $c$  and  $D$  bands for  $p_T < 10$  GeV, bands narrow for sufficiently large  $p_T$

Larger uncertainty bands for  $c$  and  $D$  than  $b$  and  $B$

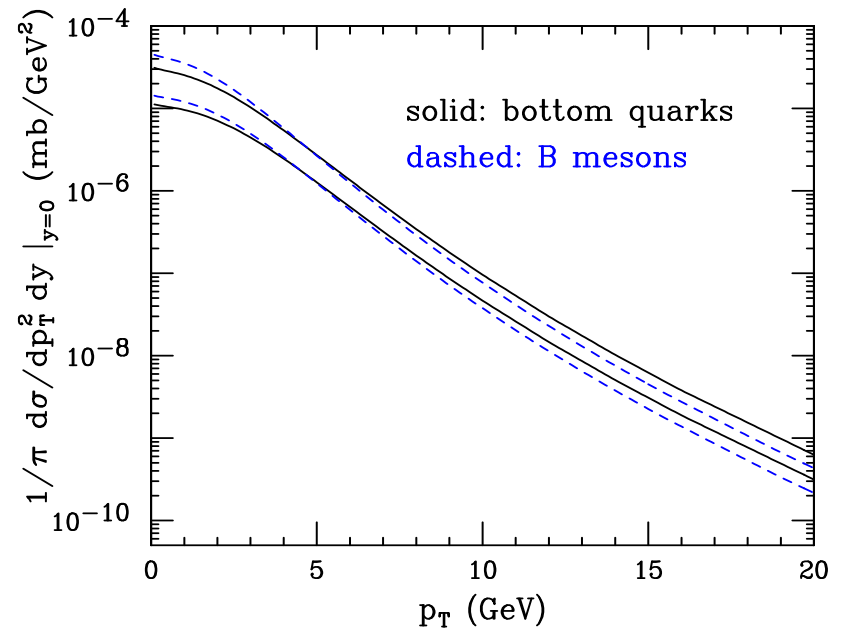
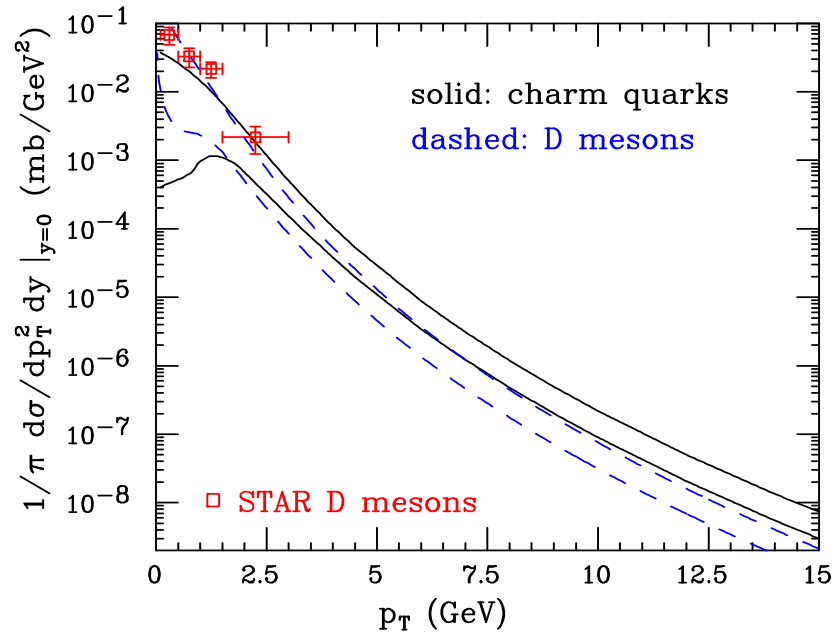


Figure 12: Left-hand side: The theoretical uncertainty bands for  $c$  quark and  $D$  meson  $p_T$  distributions in  $pp$  collisions at  $\sqrt{s} = 200$  GeV, using  $\text{BR}(c \rightarrow D) = 1$ . The final STAR d+Au data (scaled to  $pp$  using  $N_{\text{coll}} = 7.5$ ) are also shown. Right-hand side: The same for  $b$  quarks and  $B$  mesons.

# Obtaining the Electron Spectra From Heavy Flavor Decays

$D$  and  $B$  decays to leptons depends on measured decay spectra and branching ratios

$D \rightarrow e$  Use preliminary CLEO data on inclusive electrons from semi-leptonic  $D$  decays, assume it to be indentical for all charm hadrons

$B \rightarrow e$  Primary  $B$  decays to electrons measured by Babar and CLEO, fit data and assume fit to work for all bottom hadrons

$B \rightarrow D \rightarrow e$  Obtain electron spectrum from convolution of  $D \rightarrow e$  spectrum with parton model calculation of  $b \rightarrow c$  decay

Branching ratios are admixtures of charm and bottom hadrons

$$B(D \rightarrow e) = 10.3 \pm 1.2\%$$

$$B(B \rightarrow e) = 10.86 \pm 0.35\%$$

$$B(B \rightarrow D \rightarrow e) = 9.6 \pm 0.6\%$$

# Uncertainty Bands for Electrons from Heavy Flavor Decays at 200 GeV

Electrons from  $B$  decays begin to dominate at  $p_T \sim 5$  GeV

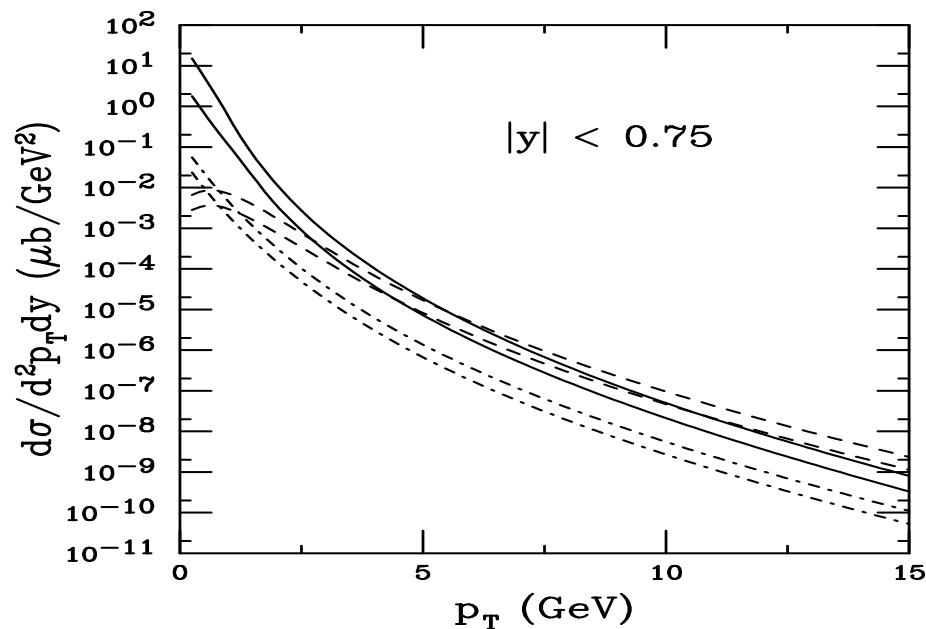


Figure 13: Left-hand side: The theoretical uncertainty bands for  $D \rightarrow e$  (solid),  $B \rightarrow e$  (dashed) and  $B \rightarrow D \rightarrow e$  (dot-dashed) as a function of  $p_T$  in  $\sqrt{s} = 200$  GeV  $pp$  collisions for  $|y| < 0.75$ . Right-hand side: The final electron uncertainty band in  $pp$  collisions is compared to the PHENIX and STAR (final and preliminary data).

# Location of $b/c$ Crossover Sensitive to Details of Fragmentation Scheme, Scales, Quark Mass

The  $b \rightarrow e$  decays dominate already at lower  $p_T$  when standard Peterson function fragmentation ( $\epsilon_c = 0.06, \epsilon_b = 0.006$ ) is used since it hardens charm  $p_T$  spectra more than bottom

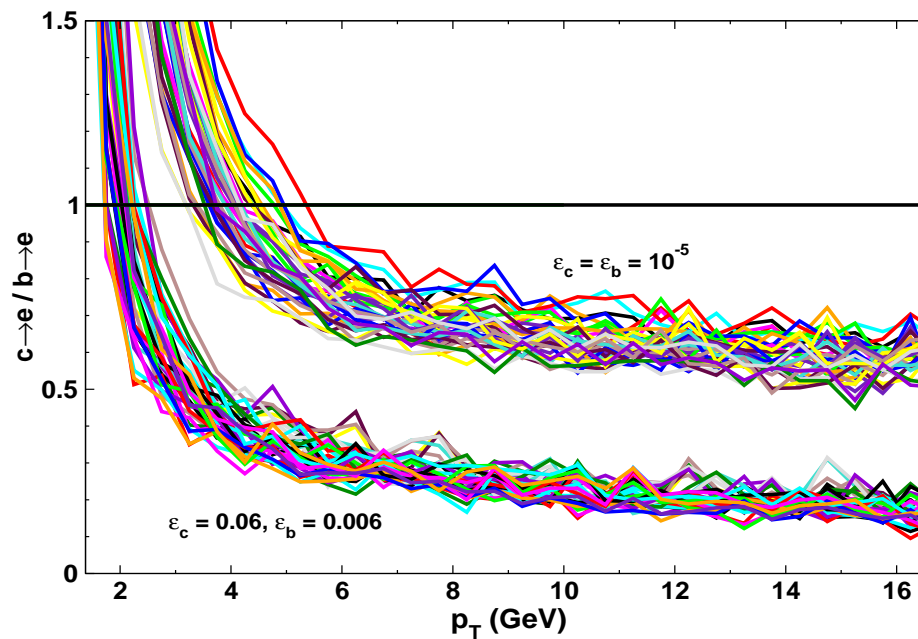


Figure 14: The ratio of charm to bottom decays to electrons obtained by varying the quark mass and scale factors. The effect of changing the Peterson function parameters from  $\epsilon_c = 0.06, \epsilon_b = 0.006$  (lower band) to  $\epsilon_c = \epsilon_b = 10^{-5}$  (upper band) is also illustrated. (From M. Djordjevic *et al.*)

# Comparison to Electron Data at 200 GeV

PHENIX  $pp$  data near top of uncertainty range over all  $p_T$ , like other experiments, e.g. at the Tevatron

STAR preliminary data/FONLL ratio  $\sim 3 - 5$ , published ratio even higher

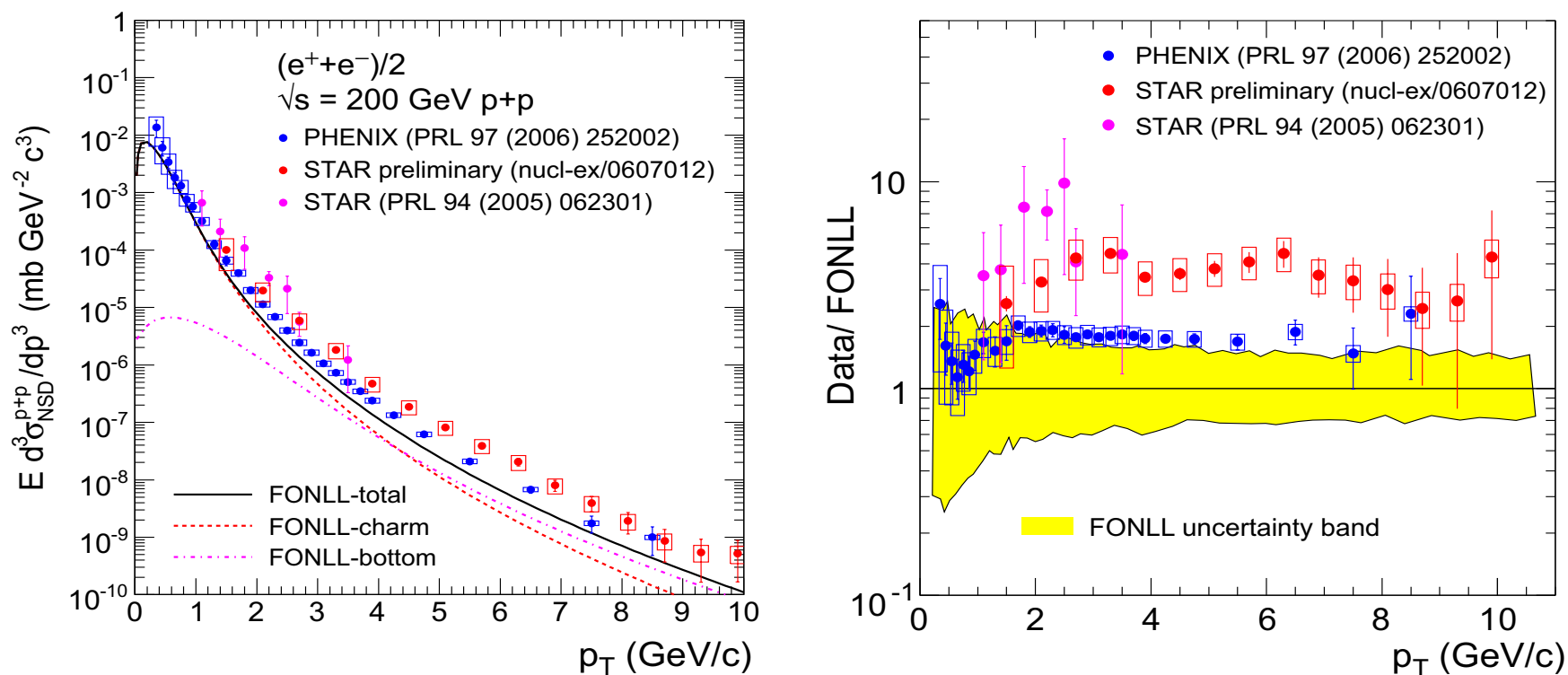


Figure 15: Left: Compilation of PHENIX and STAR measurements of the  $p_T$  dependence of the semileptonic decay open heavy flavor cross section from 200 GeV  $pp$  collisions, compared with FONLL calculations at central  $m$ ,  $\mu$  values. Right: The ratio of the data to the FONLL calculation. The band depicts the theoretical uncertainty of the calculation.

# Summary

- Total charm cross sections have large experimental and theoretical uncertainties
- More massive bottom quarks behave better
- PYTHIA and NLO calculations give similar  $\sqrt{S}$  dependence for total charm cross sections (but PYTHIA gives higher total for same mass and scale) and same basic shape for most differential distributions but only if PYTHIA parameters tuned properly – Care needed in interpretation, not different mechanisms than NLO, just different PYTHIA implementation
- At RHIC, STAR and PHENIX measure same shape for single electron spectra in  $pp$  and  $d+Au$ , agrees with FONLL prediction, difference lies in normalization: the issue still needs to be resolved
- Shape of single electron spectra changes in  $Au+Au$  collisions, caused by energy loss of fast partons in matter, results like those for light quarks – may imply that either charm and bottom quarks lose energy like light quarks or charm loses energy like light quarks and bottom is unimportant – answer depends on resolving  $pp$  discrepancy between experiments